A Neuro-Adaptive Variable Structure Control for Partially Unknown Nonlinear Dynamic Systems and Its Application

Chih-Lyang Hwang and Cheng-Ye Hsieh

***Abstract*—If the unknown nonlinear dynamic system is not in a controllable canonical form or of relative degree one, then the derivative of the tracking error is unknown. The controller design for these systems will be complex. In this paper, an estimator for the unknown tracking error with order equivalent to relative degree, is first designed, to obtain a sliding surface and to reduce the number of unknown nonlinear functions required to learn. In this situation, the total number of connection weight in neural-networks decreases. Furthermore, two learning laws with e-modification are employed to ensure the boundedness of estimated connection weights without the requirement of persistent excitation (PE) condition. The system performance can be better than that of other control schemes required many learning functions. In addition, stability of the overall system is verified by Lyapunov theory so that ultimate bounded tracking is accomplished. Simulation and experimental results of four-bar-linkage system are presented to confirm the usefulness of the proposed control.**

***Index Terms*—Four-bar-linkage system, Lyapunov stability, neuro-adaptive control, state estimator, variable structure control.**

I. Introduction

IT IS well known that learning is a first step toward the intelligent control. Learning has the capability of reducing the uncertainties affecting the performance of a dynamic system through system identification, thereby enhancing the knowledge about the system so that it can be controlled more effectively. One of the important intelligent control structures is identification-based neural-network control. Considerable research has been devoted to identification-based neural-network control or modeling structures [1]–[10]. Each study has its own advantages and disadvantages.

The current paper deals with a class of unknown affine nonlinear dynamic systems that are not necessary in controllable canonical form or that have relative degree larger than one [11]. First, an estimator for the unknown tracking error with order equivalent to relative degree, is designed to attain a sliding surface and to reduce the number of unknown nonlinear functions required to learn. Therefore, the total number of connection weights in the neural-networks decreases as compared with the other learning schemes (e.g., [4] and [5]). Furthermore, two learning laws with e-modification are considered to guarantee the boundedness of the connection weights, without the requirement of PE condition. A suitable selection of learning and e-modification rates can result in a better transient response and effective learning of unknown functions [10].

Manuscript received July 22, 2000. Manuscript received in final form May 22, 2001. Recommended by Associate Editor S. Nair. This work was supported by the National Science Council of R.O.C. under Grant NSC-87-2218-E-036-001.

The authors are with the Department of Mechanical Engineering of Tatung University, Taipei, Taiwan 10451, R.O.C. (e-mail: clhwang@ttu.edu.tw).

Publisher Item Identifier S 1063-6536(02)00088-X.

Due to the advantages of variable structure control (e.g., fast response, invariance properties [3], [7], [13], [14]), a neural-network-based variable structure control is constructed to improve the system performance. Then the stability of the overall system, including the controlled system, the estimator of tracking error, and the neural-network-based variable structure control, is verified by Lyapunov theory. Finally, the simulations and experiments for velocity control of the four-bar-linkage system are presented to confirm the usefulness of the proposed controller. As compared with the previous studies (e.g., [4] and [5]), the proposed control is simple and effective. It is believed that the proposed control can be applied to many control systems.

II. Problem Formulation

Consider the following class of partially unknown nonlinear dynamic systems:

$$\dot{x}(t) = A(x) + B(x)u(t), \qquad y(t) = C(x) \tag{1}$$

where $x(t) \in \Re^n$ denotes the system state which is available; $y(t)$ and $u(t) \in \Re$ represent the system output and input; the vectors $A(x)$, $B(x)$ and the scalar $C(x)$ are unknown mappings: $\Re^n \to \Re^n$ and $\Re^n \to \Re$, respectively. The system (1) is assumed reachable around x_0 and observable at $x_0 \in X$. However, it is not necessary to assume a controllable canonical form and a relative degree one [11]. The system (1), with the relative degree m, is defined as follows:

$$y^{(i)}(t) = L_A^i C(x), \qquad 0 \le i \le m-1,\ L_A^0 C(x) = C(x) \tag{2a}$$

$$y^{(m)}(t) = L_A^m C(x) + L_B L_A^{m-1} C(x) u(t)$$
$$L_B L_A^{m-1} C(x) \neq 0 \tag{2b}$$

where $L_A^m C(x)$ and $L_B L_A^{m-1} C(x)$ denote the Lie derivatives of the scalar $C(x)$ in the direction of the vector fields $A(x)$ and $B(x)$ with relative degree m [15], [16]. Define the following tracking error signals:

$$\begin{aligned} e_1(t) &= y(t) - r(t) \\ e_2(t) &= \dot{y}(t) - \dot{r}(t), \ \ldots \\ e_m(t) &= y^{(m-1)}(t) - r^{(m-1)}(t) \end{aligned} \tag{3}$$

where $r(t)$, $\dot{r}(t)$, $\ldots$, and $r^{(m-1)}(t)$ represent the known and bounded reference input up to $m-1$ derivatives. Because the signals $\dot{y}(t), \ldots, y^{(m-1)}(t)$ are unknown, the tracking error signals $e_2(t), \ldots, e_m(t)$ should be estimated. First, (2) and (3) are rewritten as follows:

$$\dot{E}(t) = \overline{A}E(t) + \overline{B}\left[L_A^m C(x) + L_B L_A^{m-1} C(x) u(t) - r^{(m)}(t)\right] \tag{4a}$$

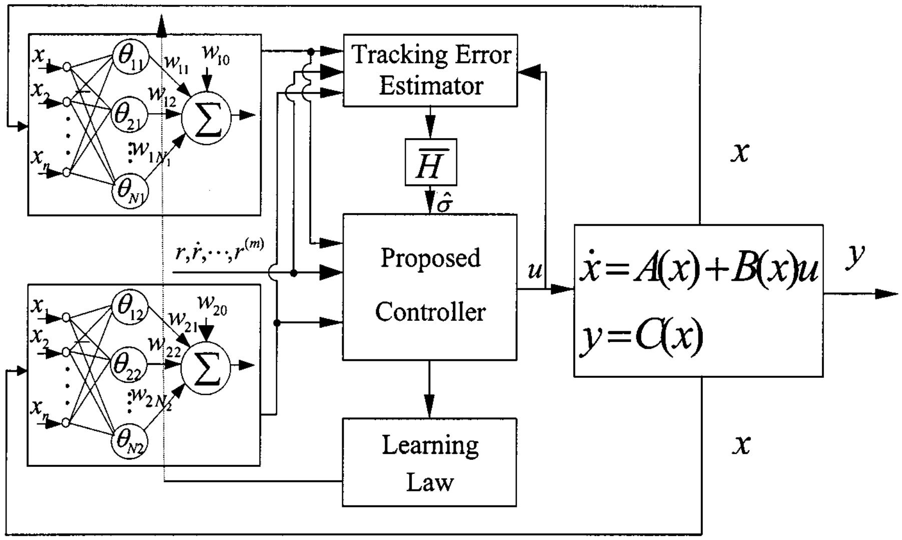

Fig. 1. Control block diagram.

where

$$\overline{A} = \begin{bmatrix} 0 & 1 & & \\ \vdots & & \ddots & \\ & & & 1 \\ 0 & \dots & & 0 \end{bmatrix}, \quad \overline{B} = \begin{bmatrix} 0 \\ \vdots \\ 0 \\ 1 \end{bmatrix}$$

$$E(t) = [\, e_1(t) \quad e_2(t) \quad \cdots \quad e_m(t)\,]^T. \tag{4b}$$

It is assumed that the unknown scalar signals $L_A^m C(x)$ and $L_B L_A^{m-1} C(x)$ can be smoothly truncated outside of $x(t) \in \Omega(x)$ (a compact subset in $\Re^n$). Hence, their spatial Fourier transformations are absolutely integrable. Based on the universal approximation theory (e.g., [2], [3], [9]), they are approximated by the following radial basis function neural-network (RBFN):

$$L_A^m C(x) = \overline{W}_1^T \Theta_1(x) + \overline{\varepsilon}_1(x),$$
$$L_B L_A^{m-1} C(x) = \overline{W}_2^T \Theta_2(x) + \overline{\varepsilon}_2(x) \tag{5a}$$

where

$$\overline{W}_i = [\, \overline{w}_{10} \quad \overline{w}_{11} \quad \cdots \quad \overline{w}_{1N_i}\,]^T$$
$$\|\overline{W}_i\| \le W_{im} \tag{5b}$$
$$\Theta_i(x) = [\, 1 \quad \theta_1(x) \quad \cdots \quad \theta_{N_i}(x)\,]^T \tag{5c}$$
$$\theta_i(x) = \exp[-\|x(t) - c_i\|^2 / \sigma_i^2]$$
$$i = 1, 2, \ldots, N_1 \text{ or } N_2 \tag{5d}$$
$$|\overline{\varepsilon}_i(x)| \le \varepsilon, \qquad i = 1, 2. \tag{5e}$$

The information about $\varepsilon, c_i, \sigma_i, N_j, W_{jm}$ for $i = 1, 2, \ldots, N_j$, $j = 1, 2$ is known. Furthermore

$$\overline{W}_2^T \Theta_2(x) > L_{2l} \gg \varepsilon > 0 \tag{6}$$

where L_{2l} is known. In fact, ε is regarded as the summation of the class membership error, the aliasing error and the truncation error [3]. The centers c_i for $i = 1, 2, \ldots, N_j$ and $j = 1, 2$ are chosen as a normal distribution in the domain $\Omega(x)$. The larger the value of variance σ_i^2 for $i = 1, 2, \ldots, N_j$ and $j = 1, 2$, is selected, the smoother $\theta_i(x)$ is around the corresponding center c_i. The problem is to develop a neuro-adaptive variable structure control for a class of unknown nonlinear dynamic systems (1) to track a time-varying trajectory (see Fig. 1).

III. Controller Design

There are three sections discussing the controller design. To estimate the unknown signal $E(t)$, a state estimator driving by the first component of $\tilde{E}(t)$ [i.e., $\tilde{e}_1(t) = e_1(t) - \hat{e}_1(t)$ which is available] is designed. The second section examines the bounded tracking result theoretically. The main theorem of neuro-adaptive variable structure control is reported in the final section.

A. Estimator for Unknown Signal

The following state estimator is designed to estimate the signal $E(t)$:

$$\dot{\hat{E}}(t) = \overline{A}\hat{E}(t) + \overline{DC}\left[E(t) - \hat{E}(t)\right] + \overline{B}\left\{\left[\hat{W}_1^T(t)\Theta_1(x)\right] + \left[\hat{W}_2^T(t)\Theta_2(x)\right]u(t) - r^{(m)}(t)\right\} \tag{7}$$

where $\hat{E}(t) = [\, \hat{e}_1(t) \quad \hat{e}_2(t) \quad \cdots \quad \hat{e}_m(t)\,]^T$ denotes the estimate of $E(t)$, $\overline{D} = [\, d_1 \quad d_2 \quad \cdots \quad d_m\,]^T$, $\overline{C} = [\, 1 \quad 0 \quad \cdots \quad 0\,]$ and $\hat{W}_i(t)$ represents the learning $\overline{W}_i$ for $i = 1, 2$. Subtracting (4a) and (4b) from (7), and using (5a)–(5e) gives

$$\dot{\tilde{E}}(t) = D\tilde{E}(t) + \overline{B} \cdot \left\{\tilde{W}_1^T(t)\Theta_1(x) + \overline{\varepsilon}_1(x) + \left[\tilde{W}_2^T(t)\Theta_2(x) + \overline{\varepsilon}_2(x)\right]u(t)\right\} \tag{8a}$$

where

$$D = \begin{bmatrix} -d_1 & 1 & & \\ \vdots & & \ddots & \\ & & & 1 \\ -d_2 & & & 0 \end{bmatrix}, \qquad \tilde{E}(t) = E(t) - \hat{E}(t),$$
$$\tilde{W}_i(t) = \overline{W}_i - \hat{W}_i(t), \qquad i = 1, 2. \tag{8b}$$

One can select the gains of the state estimator d_i for $i = 1, 2, \ldots, m$ such that D is Hurwitz. Given a positive definite symmetric matrix F (denoted as $F > 0$), there exists a unique matrix $G > 0$ such that the following Lyapunov matrix equation (9) is satisfied:

$$D^T G + GD = -F. \tag{9}$$

Remark 1: If the estimator (7) is not employed to obtain the unknown tracking error $E(t)$, some extra neural networks should be used to approximate the signal $E(t)$ (e.g., [5] and [6]). Under these circumstances, the number of estimated connection weights increases extremely. Then the convergent rate of the closed-loop signal becomes sluggish and the instability of closed-loop system probably occurs [2]–[11]. If $m = 1$, the estimator (7) is not needed. Hence, the stability of the closed-loop system becomes simple to analyze.

B. Ultimately Bounded Tracking

A sliding surface is defined as follows:

$$\sigma(t) = \overline{H}E(t) \tag{10}$$

where $\overline{H} = [h_{m-1} \quad \cdots \quad h_1 \quad 1]$. Or $E(t) = \overline{H}^p \sigma(t)$, where $\overline{H}^p = \overline{H}(\overline{H}\overline{H}^T)^{-1}$. The coefficients h_i for $i = 1, 2, \ldots, m-1$ are chosen such that $\sigma(t) = 0$ is Hurwitz. Rearrange (10) as follows:

$$\dot{\overline{E}}(t) = H\overline{E}(t) + \overline{B}\sigma(t) \tag{11a}$$

where

$$H = \begin{bmatrix} 0 & 1 & & \\ & & \ddots & \\ & & & 1 \\ -h_{m-1} & \cdots & & -h_1 \end{bmatrix}$$
$$\overline{E}(t) = [e_1(t) \quad e_2(t) \quad \cdots \quad e_{m-1}(t)]^T. \tag{11b}$$

The following lemma discusses the stability of (11a) and (11b) when $\sigma(t) \neq 0$ and $|\sigma(t)|$ is small.

Lemma 1 [11]: If the dynamics of the sliding surface (11a) and (11b) satisfies the following inequality $|\sigma(t)| \le \alpha$ for $t \ge t_0$, then $\|\overline{E}(t)\| < K_1\alpha/K_2$, where $\|\exp[H(t-t_0)]\| \le K_1 \exp[-K_2(t-t_0)]$, $\forall t \ge t_0 \ge 0$.

C. Neuro-Adaptive Variable Structure Control

First, the estimated sliding surface is defined as follows:

$$\hat{\sigma}(t) = \overline{H}\hat{E}(t). \tag{12}$$

Two update laws for connection weights are designed as follows:

$$\dot{\hat{W}}_1(t) = \hat{\sigma}(t)\Gamma_1\Theta_1(x) - \eta_1\Gamma_1\hat{W}_1(t) \tag{13a}$$
$$\dot{\hat{W}}_2(t) = \hat{\sigma}(t)u_{eq}(t)\Gamma_2\Theta_2(x) - \eta_2\Gamma_2\hat{W}_2(t) \tag{13b}$$

where $\Gamma_i = \text{diag}\{\gamma_{ii}\}$, $\gamma_{ii} > 0$, $\eta_i > \lambda > 0$ for $i = 1, 2$ and $u_{eq}(t)$ is described in (14b). Let

$$u(t) = u_{eq}(t) + u_{sw}(t) \tag{14a}$$

where

$$u_{eq}(t) = \left\{r^{(m)}(t) - \overline{HA}\hat{E}(t) - \hat{W}_1^T(t)\Theta_1(x)\right\}/L_{eq}(t) \tag{14b}$$

$$L_{eq}(t) = \begin{cases} \hat{W}_2^T(t)\Theta_2(x), & \text{if } \hat{W}_2^T(t)\Theta_2(x) > L_{2l} \\ L_{2l}, & \text{otherwise} \end{cases} \tag{14c}$$

$$u_{sw}(t) = -[\xi_1\hat{\sigma}(t) + \xi_2\hat{\sigma}(t)/|\hat{\sigma}(t)|]/(L_{2l} - \varepsilon) \tag{14d}$$

where $\xi_1, \xi_2 > 0$. The following lemma examines the upper bound of the proposed control.

Lemma 2: Because $|r^{(m)}(t)| \le r_m \forall t$, the proposed controller is then bounded by (15a)–(15d)

$$|u_{eq}(t)| \le k_0 + k_1|\sigma(t)| + k_2\|\tilde{W}_1(t)\| + k_3\|\tilde{E}(t)\| \tag{15a}$$
$$|u_{sw}(t)| \le k_4 + k_5|\sigma(t)| + k_6\|\tilde{E}(t)\| \tag{15b}$$

where

$$k_0 = \left(r_m + W_{1m}\sqrt{N_1}\right)/L_{2l}, \qquad k_1 = \left\|\overline{HA}\overline{H}^p\right\|/L_{2l}$$
$$k_2 = \sqrt{N_1}/L_{2l}, \qquad k_3 = \left\|\overline{HA}\right\|/L_{2l} \tag{15c}$$
$$k_4 = \xi_2/(L_{2l} - \varepsilon), \qquad k_5 = \xi_1/(L_{2l} - \varepsilon)$$
$$k_6 = \xi_1\left\|\overline{H}\right\|/(L_{2l} - \varepsilon). \tag{15d}$$

Proof: Substituting (12), (8a), (8b), (5a)–(5e) into (14b) and (14d), and using the triangle inequality (e.g., $\|\hat{W}_1(t)\| \le \|\overline{W}_1\| + \|\tilde{W}_1(t)\| \le W_{1m} + \|\tilde{W}_1(t)\|$, $\|\hat{E}(t)\| \le \|E(t)\| + \|\tilde{E}(t)\| \le \|\overline{H}\||\sigma(t)| + \|\tilde{E}(t)\|$ and $|\hat{\sigma}(t)| \le |\sigma(t)| + |\tilde{\sigma}(t)| \le |\sigma(t)| + \|\overline{H}\|\|\tilde{E}(t)\|$), give the results.

Theorem 1: Consider the nonlinear dynamic system (1) and the controller (12)–(14), and (7) with $\hat{W}_2(t_0) \ge L_{2l}$. The domain $\Omega(x)$ is chosen large enough for the learning of $L_A^m C(x)$ and $L_B L_A^{m-1} C(x)$. The overall system $Z(t) = [\sigma(t) \quad \tilde{W}_1^T(t) \quad \tilde{W}_2^T(t) \quad \tilde{E}^T(t)]^T \in \Omega'(Z) \subset \Re^{n_z}$, $n_z = N_1 + N_2 + m + 3$ and $Z(t_0) \in B_r(Z) \subset \Omega'(Z)$. The following inequalities are satisfied:

$$\xi_1 > \varepsilon k_1 + \lambda, \qquad \xi_2 > \varepsilon(1 + k_0)$$

and

$$\lambda_{\min}(F) > \left[\xi_1\left\|\overline{H}\right\|^2 + 2\varepsilon(k_3 + k_6)\|G\|\right] + \lambda \tag{16a}$$

such that

$$\begin{aligned} q(t) = &(\xi_1 - \varepsilon k_1 - \lambda) \\ &\cdot [(\eta_1 - \lambda)(\eta_2 - \lambda)\phi_{44} - (\eta_1 - \lambda)\phi_{34}^2 - (\eta_2 - \lambda)\phi_{24}^2] \\ &+ [\phi_{12}^2\phi_{34}^2 + 2(\eta_2 - \lambda)\phi_{12}\phi_{14}\phi_{24} - (\eta_1 - \lambda)(\eta_2 - \lambda)\phi_{14}^2 \\ &- (\eta_2 - \lambda)\phi_{44}\phi_{12}^2] > 0 \end{aligned} \tag{16b}$$

where

$$\begin{aligned} \phi_{11} &= \xi_1 - \varepsilon k_1 - [\varepsilon(1 + k_0) - \xi_2]/|\sigma(t)| \\ \phi_{12} &= -\varepsilon k_2/2, \qquad \phi_{13} = 0 \\ \phi_{14} &= -\left\{\left\|\overline{HA}\right\| + 2\xi_1\left\|\overline{H}\right\| + \varepsilon k_2 + 2\varepsilon(k_0 + k_5)\|G\|\right\}/2 \\ \phi_{22} &= \eta_1, \qquad \phi_{23} = 0 \\ \phi_{24} &= -\left\{\left\|\overline{H}\right\|\sqrt{N_1} + 2\|G\| \left[\sqrt{N_1} + \varepsilon k_2 + \sqrt{N_2}(k_0 + k_4)\right]\right\}/2 \\ \phi_{33} &= \eta_2, \qquad \phi_{34} = -k_0\left\|\overline{H}\right\|\sqrt{N_2}/2 \\ \phi_{44} &= \lambda_{\min}(F) - \left[\xi_1\left\|\overline{H}\right\|^2 + 2\varepsilon(k_3 + k_6)\|G\|\right]. \end{aligned} \tag{16c}$$

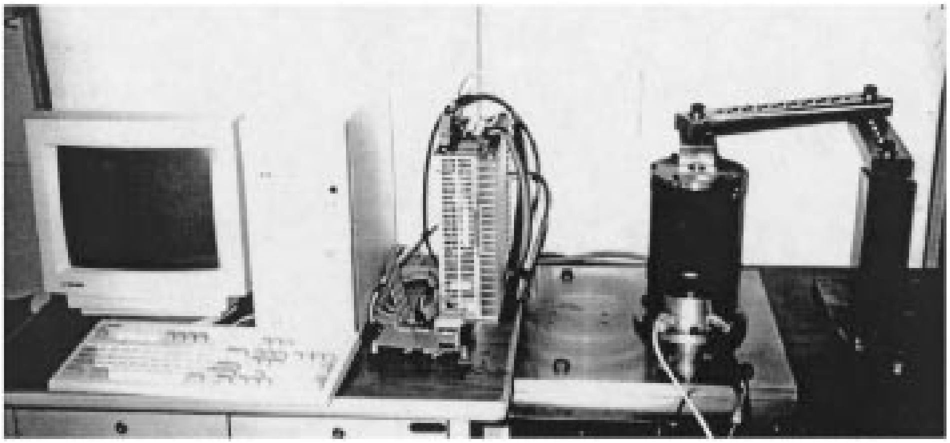

Fig. 2. Experimental setup.

Then $\{\hat{\sigma}(t), \hat{W}_1(t), \hat{W}_2(t), \hat{E}(t), u(t)\}$ are bounded and the system performance satisfies

$$\lim_{t\to\infty} Z(t) \in \overline{\Omega} = \{Z \in \Omega' | (\Phi - \lambda I)Z_n - \Psi \leq 0\} \quad (17)$$

where $\Phi(\sigma)$ is a 4×4 symmetric matrix with the entries in (16c)

$$Z_n(t) = \left[|\sigma(t)| \quad \left\|\tilde{W}_1(t)\right\| \quad \left\|\tilde{W}_2(t)\right\| \quad \left\|\tilde{E}(t)\right\| \right] \quad (18)$$

$$\Psi(Z_n) = [0 \quad \eta_1 W_{1m} \quad \eta_2 W_{2m} \quad \varphi_4(Z_n)]^T \quad (19)$$

$$\begin{aligned}\varphi_4(Z_n) =& \xi_2 \left\|\overline{H}\right\| + 2\varepsilon\|G\|(1+k_0+k_4) + \left\|\overline{H}\right\| \sqrt{N_2} \left\|\tilde{W}_2(t)\right\| \\ &\cdot \left[k_1|\sigma(t)| + k_2 \left\|\tilde{W}_1(t)\right\| + k_3 \left\|\tilde{E}(t)\right\|\right] \\ &+ 2\|G\|\sqrt{N_2} \left\|\tilde{W}_2(t)\right\| \\ &\cdot \left[(k_1+k_5)|\sigma(t)| + k_2 \left\|\tilde{W}_1(t)\right\| + (k_3+k_6) \left\|\tilde{E}(t)\right\|\right].\end{aligned} \quad (20)$$

Furthermore, the tracking performance bound is $\|\overline{E}(t)\| < K_1\alpha/K_2$, if the signal $|\sigma(t)|$ in $\overline{\Omega}$ satisfies $|\sigma(t)| \leq \alpha$.

Proof: See Appendix A.

Remark 2: The condition (16a)–(16c) implies that the gain of the switching control (i.e., ξ_1, ξ_2) must be selected large enough to deal with the uncertainties (i.e., ε) connected with the equivalent control (i.e., k_0, k_1). It also implies that the minimum eigenvalue of estimator [i.e., $\lambda_{\min}(F)$] must be chosen large enough to cope with the uncertainties (i.e., ε) and the switching gain (i.e., ξ_1). However, too large eigenvalues of the estimator probably result in poor transient response.

Remark 3: If the control input is not smooth enough, the modification for $u_{sw}(t)$ can be

$$u_{sw}(t) = -\{\xi_1\hat{\sigma}(t) + \xi_2\hat{\sigma}(t)/[|\hat{\sigma}(t)| + \mu]\}/(L_{2l} - \varepsilon) \quad (21)$$

where μ is a small positive constant.

IV. Simulations and Experiments of Four-Bar-Linkage Systems

A. Experimental Setup

The four-bar-linkage system hardware mainly consists of five parts: a direct-drive motor, a driver, a four-bar-linkage, an AD/DA card and a personal computer (see Fig. 2). The specifications of direct-drive motor are briefly introduced as follows: rate speed 12.56 rad/s, maximum output torque 7.653 kgm, power consumption 1.6 KVA, stiffness 9.8×10^{-7} rad/kgm and inertia $J_m = 2.7 \times 10^{-2}$ kgm. The four-bar-linkage system has the following specifications: $l_1 = 0.31$ m, $l_2 = 0.1$ m, $l_3 = 0.35$ m, $l_4 = 0.25$ m, $m_2 = 1.55$ kg, $m_3 = 4.3$ kg, $m_4 = 3.55$ kg, $I_2 = 5.8125 \times 10^{-4}$ kgm, $I_3 = 1.3125 \times 10^{-3}$ kgm and $I_4 = 1.3313 \times 10^{-3}$ kgm. Because the first linkage is fixed, the information of m_1 and I_1 is not required. The torque constant $K_t = 1.05$ kgm/amp is achieved from the maximum torque and the maximum current. The voltage conversion factor for velocity and current are 0.55 rad/s/voltage and 1.153×10^{-2} amp/voltage, respectively. After sampling by a 12-bit A/D card (e.g., PCL-1800), the resolution of velocity and current is 2.686×10^{-3} rad/s and 5.63×10^{-5} amp, respectively. The control cycle time for the proposed algorithm is 0.01 s.

B. System Analysis

The threshold voltage of direct-drive motor with four-bar-linkage is about 1.15 *voltage*. As compared with only direct-drive motor inertia, the system with linkage load needs more power and its static friction torque also increases. Moreover, the sinusoidal response with the four-bar-linkage load in Fig. 3 reveals that the proposed system contains complex and time-varying nonlinearities. The responses for different PID control gains are not good; those are omitted due to the space limits. That is, the only use of PID control cannot achieve an excellent tracking result. This is one of the important motivations for the present study.

C. Simulations

The dynamics of the four-bar-linkage driven by a direct-drive motor in a horizontal plane through a rigid coupling are described by the following equations:

$$L_m \dot{i}_m(t) + R_m i_m(t) + K_b \dot{\theta}_m(t) = E_a(t) \tag{22a}$$

$$M_e(\theta_2)\ddot{\theta}_2(t) + (B_m + B_l)\dot{\theta}_2(t) + C_b(\theta_2)\dot{\theta}_2^2(t) + T_{un}(E_a, \dot{\theta}_2) = T_m(t) = K_t i_m(t) \tag{22b}$$

$$\theta_2(t) = \theta_m(t), \quad \dot{\theta}_2(t) = \dot{\theta}_m(t), \quad \ddot{\theta}_2(t) = \ddot{\theta}_m(t) \tag{22c}$$

where the symbols $M_e(\theta_2)$, $(B_m + B_l)$, $C_b(\theta_2)$, and $T_{un}(E_a, \dot{\theta}_2)$ denote effective inertia, linear damping of motor and load, centrifugal and Coriolis, and unmodeled dynamics included friction, disturbance and external torque, respectively. The symbols L_m, R_m, K_b, $i_m(t)$, $\theta_m(t)$, and $T_m(t)$ represent motor inductance, resistance, back-emf constant, current, angular position, and torque, respectively (see Appendix B for details). Unmodeled dynamics is assumed as the following friction torque [9], [17]:

$$T_{un}(E_a, \dot{\theta}_2) = T_{\text{slip}}(\dot{\theta}_2)\phi(\dot{\theta}_2) + T_{\text{stick}}(E_a)[1 - \phi(\dot{\theta}_2)] \tag{23}$$

where $\phi(\dot{\theta}_2) = 1$ as $|\dot{\theta}_2(t)| > \varepsilon_3$, and $\phi(\dot{\theta}_2) = 0$, otherwise. The sticking torque is modeled as follows:

$$T_{\text{stick}}(E_a) = \begin{cases} T_s^+, & K_t E_a(t)/R_m > T_s^+ > 0 \\ K_t E_a(t)/R_m, & T_s^- \le K_t E_a(t)/R_m \le T_s^+ \\ T_s^-, & K_t E_a(t)/R_m < T_s^- < 0. \end{cases} \tag{24}$$

The slipping torque is modeled as follows:

$$T_{\text{slip}}(\dot{\theta}_2) = \begin{cases} T_s^+ - \delta T^+\{1 - \exp[-|\dot{\theta}_2(t)/\dot{\theta}_2^+|]\} \\ \quad +C^+\dot{\theta}_2(t), \qquad \dot{\theta}_2(t) > 0 \\ T_s^- - \delta T^-\{1 - \exp[-|\dot{\theta}_2(t)/\dot{\theta}_2^-|]\} \\ \quad +C^-\dot{\theta}_2(t), \qquad \dot{\theta}_2(t) \le 0. \end{cases} \tag{25}$$

Rewrite the four-bar-linkage system (22a)–(22c) as the form of (1) with the following definitions:

$$[x_1(t) \quad x_2(t) \quad x_3(t)] = [\theta_2(t) \quad \dot{\theta}_2(t) \quad i_m(t)], \quad u(t) = E_a(t)$$

and

$$y(t) = x_2(t). \tag{26}$$

The system (22a)–(22c) has relative degree 2. From the measurement, $K_b = 1.05$ V/rad/s, $R_m = 1.0\ \Omega$. After a model check in Fig. 3, the following system parameters are set. Those are $\varepsilon_3 = 0.83$ rad/s $T_s^+(T_s^-) = 0.25(-0.25)$ kgm, $\delta T^+(\delta T^-) = 0.1(-0.1)$ kgm, $\dot{\theta}_2^+(\dot{\theta}_2^-) = 0.4$ rad/s, $C^+ = C^- = 0.0042$ kgms/rad, $B_m + B_l = 0.0042$ kgms/rad, and $L_m = 8.6 \times 10^{-3}$ H. The difference between the real system and mathematical model is that a rigid coupling is supposed in mathematical model. Therefore, an order reduction of (22a)–(22c) can be obtained.

Mistry *et al.* paper [5] discussed neural-network control for a similar system with two neural networks, i.e., one for identification and the other for control. Its total number of connection weights is 6050. The current paper uses $N_1 = N_2 = 126$

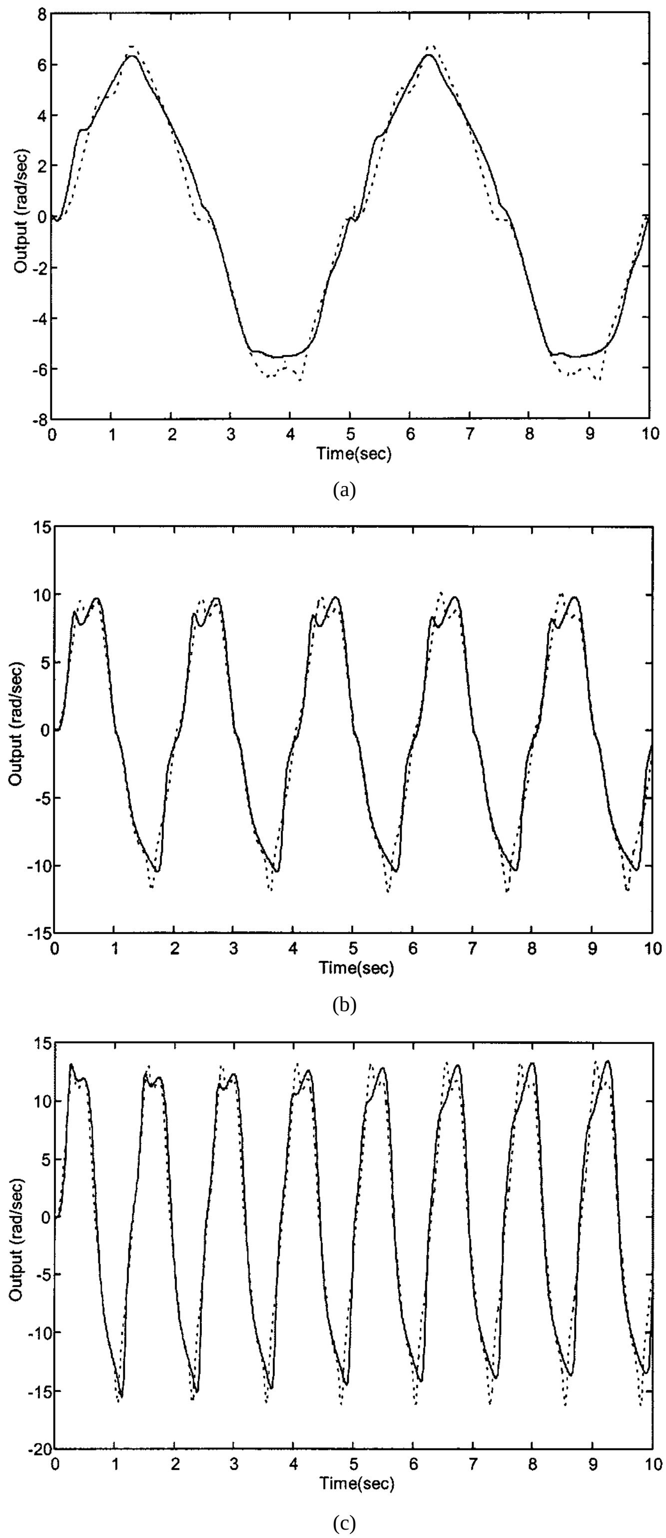

Fig. 3. Comparison of the open-loop sinusoidal responses between real system (…) and mathematical model (—) for input $u(t) = u_m \sin(2\pi f t)$ (voltage). (a) $u_m = 4,\ f = 0.2$. (b) $u_m = 6,\ f = 0.5$. (c) $u_m = 8,\ f = 0.8$.

to learn the unknown nonlinear functions $L_A^2 C(x)$ and $L_B L_A C(x)$. Due to this, the control cycle time of [5] is 43.5 ms or 83.3 ms that is four (or eight) times greater than that of the proposed control (i.e., 10 ms). The reference input is assigned as $r(t) = r_m \sin(2\pi f t)$ rad/s. A compact subset is defined as $\Omega(x) = \{x(t) | |x_1(t)| < 51.3\,\text{rad}, |x_2(t)| <$

20.52 rad/s, $|x_3(t)| < 2.5$ amp$\}$. After normalization of the state, the center of jth kernel is $c_j = [c_{j1} \quad c_{j2} \quad c_{j3}]$, where $c_{ji} \in [-1 \quad -0.5 \quad 0 \quad 0.5 \quad 1]$, and the width of jth kernel is $\sigma_j = 0.75$. The control parameters are set as $\xi_1 = 13$, $\xi_2 = 0.5$, $\mu = 0.2$, $\gamma_{11} = \gamma_{22} = 0.08$, $\eta_1 = \eta_2 = 10^{-5}$, $L_{2l} = 110$, $\varepsilon = 0.1$, $d_1 = 150$, $d_2 = 5000$, and $h_1 = 50$. The initial values of state, estimated state and connection weight are set to be zero except $\hat{w}_{20}(0) = L_{2l}$. The simulation results of the fourth process time are presented in Fig. 4. The controller can make the system output track the reference input in a satisfactory manner [see Fig. 4(a)]. The maximum tracking error occurs in the neighborhood of zero velocity because of the phenomenon of friction torque and backlash of coupling. The control input of Fig. 4(b) is smooth enough. The sliding surface and its corresponding estimated sliding surface are shown in Fig. 4(c). It indicates that the estimate $\hat{E}(t)$ is good enough for the controller design. The real nonlinear functions $L_A^2C(x)$, $L_BL_AC(x)$ and their corresponding learning neural-networks $\hat{W}_1^T(t)\Theta_1(x)$, $\hat{W}_2^T(t)\Theta_2(x)$ match each other, but not discussed here. Although the total number of connection weight is 252, they are satisfactory for the controller design. Based on the result of Fig. 4, the controller has the ability of reducing the uncertainties affecting the system performance.

D. Experiments

The initial values of state, estimated state and connection weight are the same as in the simulation case. The control parameters are set as $\xi_1 = 6$, $\xi_2 = 0.3$, $\mu = 0.2$, $\gamma_{11} = \gamma_{22} = 0.08$, $\eta_1 = \eta_2 = 10^{-5}$, $L_{2l} = 110$, $\varepsilon = 0.1$, $d_1 = 120$, $d_2 = 3200$, and $h_1 = 40$ which are a little smaller than those in simulation. Similarly, after an effective learning the typical experiment results are shown in Fig. 5. As compared with Figs. 4 and 5 and the previous study (e.g., [5]), the following conclusions are drawn: 1) The maximum tracking error for experiment case (i.e., 10.561% or 1.056 rad/s) is larger than that of simulation case (i.e., 6.824% or 0.682 rad/s) because the dynamics of real system is more complex than that of the mathematical model. In [5], for a constant desired angular speed (e.g., 3.14 rad/s) the maximum steady-state error is 28% (i.e., 0.879 rad/s) for control cycle time 83.3 ms and 20% (i.e., 0.628 rad/s) for control cycle 43.5 ms. 2) The responses of control input, sliding surface in experiment are similar with those of simulation. Again, these are omitted due to space considerations.

For verifying the usefulness of the proposed controller, the tracking for the trajectories with different frequencies is shown in Fig. 6. The maximum tracking error for lower frequency (i.e., 0.2 Hz) is 15.595% (i.e., 1.56 rad/s) that is larger than the result of 0.5 Hz case [see Fig. 5(a)]. The reason is that the friction phenomenon dominates at lower frequency [9], [17]. Similarly, the maximum tracking error for higher frequency (i.e., 0.8 Hz) is 17.544% (i.e., 1.754 rad/s) that is larger than that of 0.5 Hz case [see Fig. 5(a)]. The reason is that the phase error between system output and desired trajectory increases as the frequency of trajectory augments. The same result occurs in [5]; i.e., the steady-state errors for the desired angular speeds 1.57, 3.14, 6.28, and 15.7 rad/s cases are 178%, 25.5%, 23.9%, and 66.2% (or 2.8, 1.6, 3.0, and 10.4 rad/s), respectively.

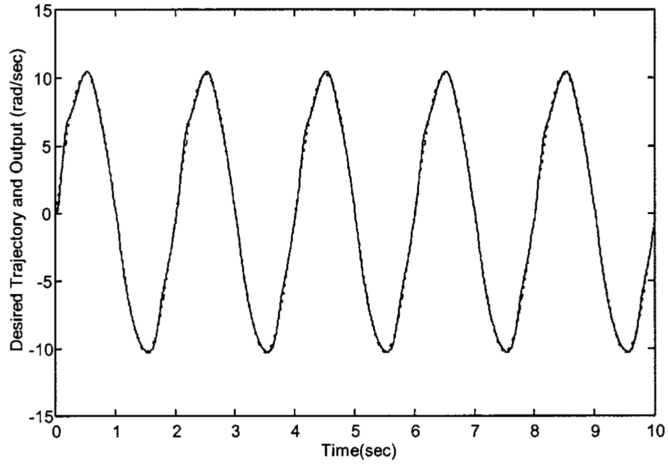

(a)

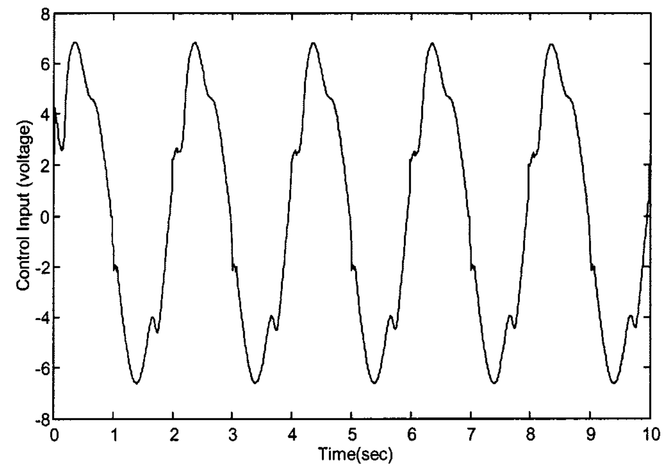

(b)

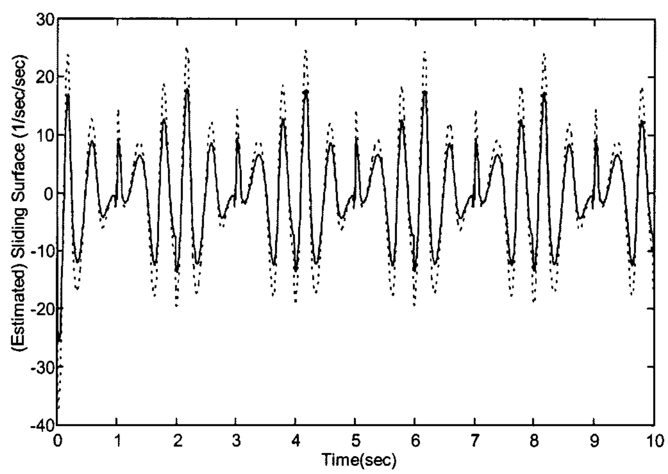

(c)

Fig. 4. Simulation results. (a) $r(t)$ (…) and $y(t)$ (—). (b) $u(t)$ (c) $\sigma(t)$ (…) and $\hat{\sigma}(t)$ (—).

Including the coupling dynamics in (22a)–(22c) will further improve performance. Another approach is to develop an integral design as done in [18].

V. Conclusion

The class of proposed nonlinear unknown system studied is not necessarily in a controllable canonical form or of relative de-

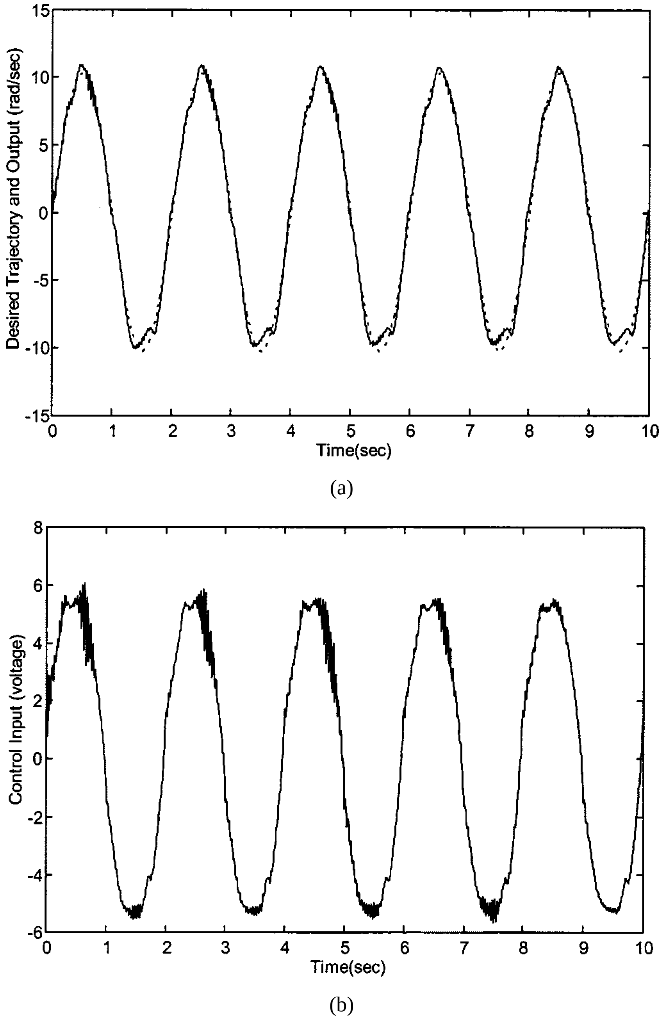

Fig. 5. Experimental results. (a) $r(t)$ (…) and $y(t)$(—). (b) $u(t)$.

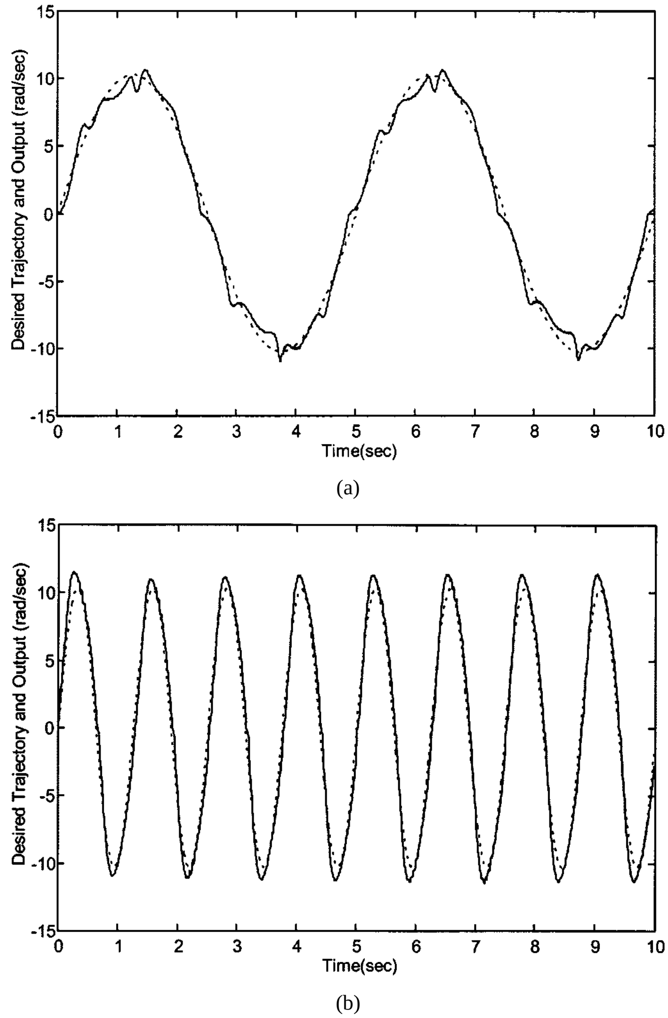

Fig. 6. The output responses of the proposed control for different frequencies. (a) $r(t)$ (…) and $y(t)$ (—) for $f = 0.2$. (b) $r(t)$ (…) and $y(t)$ (—) for $f = 0.8$.

gree one. An estimator for the tracking error is designed to obtain a sliding surface and to decrease the number of unknown nonlinear functions required to learn. The total number of connection weights in the neural-network then reduces. In addition, two learning laws with e-modification are employed to learn two Lie derivative functions with relative degree m. Explicit expression for the control parameters are also reported. Using an information of nominal system or an iterative learning of the controlled system can improve system performance. Stability of the overall system including the dynamics of the state estimator, the learning law for connection weights and trajectory tracking, is proved using Lyapunov stability theory. Simulations and experiments with a four-bar-linkage system confirm the usefulness of the proposed controller. The proposed control scheme can also be applied to other systems belonging to the same class of nonlinear systems.

Appendix A
The Proof of Theorem 1

Define the following Lyapunov function:

$$V(Z) = \left(\sigma^2 + \sum_{i=1}^{2} \tilde{W}_i^T \Gamma_i^{-1} \tilde{W}_i\right) \Big/ 2 + \tilde{E}^T G \tilde{E} = Z^T M Z \qquad \text{(A1)}$$

where $M = \operatorname{diag}[1/2 \quad \Gamma_1^{-1}/2 \quad \Gamma_2^{-1}/2 \quad G] \in \Re^{n_z \times n_z}$, $V(Z) > 0$ as $Z \neq 0$. Taking the time derivative of (A1) gives

$$\dot{V} = \sigma\dot{\sigma} - \sum_{i=1}^{2} \tilde{W}_i^T \Gamma_i \dot{\hat{W}}_i + \dot{\tilde{E}}^T G \tilde{E} + \tilde{E}^T G \dot{\tilde{E}}. \qquad \text{(A2)}$$

Substituting (1), (4a), (5a), (8a), (8b), (10), and (13a) and (13b) into (A2) gives

$$\begin{aligned}\dot{V} = {} & \overline{H}\left(\hat{E} + \tilde{E}\right) \\ & \cdot \left\{\overline{H}\left[\overline{A}E + \overline{B}\left[\overline{W}_1^T\Theta_1 + \overline{\varepsilon}_1 + \left(\overline{W}_2^T\Theta_2 + \overline{\varepsilon}_2\right)u - r^{(m)}\right]\right]\right\} \\ & - \hat{\sigma}\tilde{W}_1^T\Theta_1 + \eta_1\tilde{W}_1^T\hat{W}_1 - \hat{\sigma}u_{eq}\tilde{W}_2^T\Theta_2 + \eta_2\tilde{W}_2^T\hat{W}_2 \\ & + \tilde{E}^T(D^T G + GD)\tilde{E} + 2\tilde{E}^T G\overline{B} \\ & \cdot \left[\tilde{W}_1^T\Theta_1 + \overline{\varepsilon}_1 + \left(\tilde{W}_2^T\Theta_2 + \overline{\varepsilon}_2\right)u\right]. \end{aligned} \qquad \text{(A3)}$$

Substituting (12), (14a), (14b), and (9) into (A3) yields

$$\begin{aligned}\dot{V} = &\left(\hat{\sigma} + \overline{H}\tilde{E}\right)\\ &\cdot \Big\{\overline{HA}\tilde{E} + \overline{HB}\\ &\quad\cdot \Big[\tilde{W}_1^T\Theta_1 + \bar{\varepsilon}_1 + \left(\tilde{W}_2^T\Theta_2 + \bar{\varepsilon}_2 + \hat{W}_2^T\Theta_2 - L_{eq}\right)u_{eq}\\ &\qquad + \left(\overline{W}_2^T\Theta_2 + \bar{\varepsilon}_2\right)u_{sw}\Big]\Big\} - \hat{\sigma}\tilde{W}_1^T\Theta_1 - \hat{\sigma}u_{eq}\tilde{W}_2^T\Theta_2\\ &+ \sum_{i=1}^{2}\eta_i\tilde{W}_i^T\hat{W}_i - \tilde{E}^TF\tilde{E} + 2\tilde{E}^TG\overline{B}\\ &\cdot \left[\tilde{W}_1^T\Theta_1 + \bar{\varepsilon}_1 + \left(\tilde{W}_2^T\Theta_2 + \bar{\varepsilon}_2\right)u\right]. \end{aligned} \tag{A4}$$

Continuous simplification of (A4) by using (8b) and (14d) and the fact $\overline{HB} = 1$ gives

$$\begin{aligned}\dot{V} =& \overline{H}\tilde{E}\Big\{\overline{HA}\tilde{E} + \Big[\tilde{W}_1^T\Theta_1 + \bar{\varepsilon}_1 + \left(\tilde{W}_2^T\Theta_2 + \bar{\varepsilon}_2\right)u_{eq}\\ &\qquad + \left(\hat{W}_2^T\Theta_2 - L_{eq}\right)u_{eq}\Big]\Big\}\\ &+ \hat{\sigma}\Big\{\overline{HA}\tilde{E} + \bar{\varepsilon}_1 + \bar{\varepsilon}_2u_{eq} + \left(\hat{W}_2^T\Theta_2 - L_{eq}\right)u_{eq}\\ &\quad - \frac{\overline{W}_2^T\Theta_2 + \bar{\varepsilon}_2}{L_{2l} - \varepsilon}\left(\xi_1\hat{\sigma} + \xi_2\hat{\sigma}/|\hat{\sigma}|\right)\Big\}\\ &+ \sum_{i=1}^{2}\eta_i\tilde{W}_i^T\left(\overline{W}_i - \tilde{W}_i\right) - \tilde{E}^TF\tilde{E} + 2\tilde{E}^TG\overline{B}\\ &\cdot\left[\tilde{W}_1^T\Theta_1 + \bar{\varepsilon}_1 + \left(\tilde{W}_1^T\Theta_1 + \bar{\varepsilon}_1\right)u\right]\\ =& \sigma\left\{\overline{HA}\tilde{E} + \bar{\varepsilon}_1 + \bar{\varepsilon}_2u_{eq} + \left(W_2^T\Theta_2 - L_{eq}\right)u_{eq}\right\}\\ &+ \overline{H}\tilde{E}\left\{\tilde{W}_1^T\Theta_1 + \tilde{W}_2^T\Theta_2u_{eq}\right\}\\ &- \left(\overline{W}_2^T\Theta_2 + \bar{\varepsilon}_2\right)\left(\xi_1\hat{\sigma}^2 + \xi_2|\hat{\sigma}|\right)\Big/(L_{2l} - \varepsilon)\\ &- \sum_{i=1}^{2}\eta_i\tilde{W}_i^T\tilde{W}_i + \sum_{i=1}^{2}\eta_i\tilde{W}_i^T\overline{W}_i\\ &- \tilde{E}^TF\tilde{E} + 2\tilde{E}^TG\overline{B}\left[\tilde{W}_1^T\Theta_1 + \bar{\varepsilon}_1 + \left(\tilde{W}_1^T\Theta_1 + \bar{\varepsilon}_1\right)u\right]. \end{aligned} \tag{A5}$$

Because $\hat{W}_2(t_0) \geq L_{2l}$ and an effective learning, $\hat{W}_2^T\Theta_2 - L_{eq} = 0$ as $t > T > 0$. Taking the norm of (A5) and using the relation $-|\hat{\sigma}| \leq -|\sigma| + |\tilde{\sigma}| \leq -|\sigma| + \|\overline{H}\|\|\tilde{E}\|$, $(\overline{W}_2^T\Theta_2 + \bar{\varepsilon}_2)/(L_{2l} - \varepsilon) < 1$ yields

$$\begin{aligned}\dot{V} \leq& |\sigma|\Big\{\|\overline{HA}\|\left\|\tilde{E}\right\| + \varepsilon + \varepsilon\\ &\quad\cdot\left(k_0 + k_1|\sigma| + k_2\left\|\tilde{W}_1\right\| + k_3\left\|\tilde{E}\right\|\right)\Big\} + \|\overline{H}\|\left\|\tilde{E}\right\|\\ &\cdot\Big\{\left\|\tilde{W}_1\right\|\sqrt{N_1} + \left\|\tilde{W}_2\right\|\sqrt{N_2}\\ &\quad\cdot\left(k_0 + k_1|\sigma| + k_2\left\|\tilde{W}_1\right\| + k_3\left\|\tilde{E}\right\|\right)\Big\}\\ &- \xi_1\sigma^2 + \xi_1\|\overline{H}\|^2\left\|\tilde{E}\right\|^2 + 2\xi_1|\sigma|\,\|\overline{H}\|\left\|\tilde{E}\right\|\\ &- \xi_2|\sigma| + \xi_2\|\overline{H}\|\left\|\tilde{E}\right\| - \sum_{i=1}^{2}\eta_i\left\|\tilde{W}_i\right\|^2\\ &+ \sum_{i=1}^{2}\eta_iW_{im}\left\|\tilde{W}_i\right\| - \lambda_{\min}(F)\left\|\tilde{E}\right\|^2 + 2\left\|\tilde{E}\right\|\|G\|\\ &\Big\{\left\|\tilde{W}_1\right\|\sqrt{N_1} + \varepsilon + \left(\left\|\tilde{W}_2\right\|\sqrt{N_2} + \varepsilon\right)\\ &\quad\cdot\left[(k_0 + k_4) + (k_1 + k_5)|\sigma| + k_2\left\|\tilde{W}_1\right\| + k_3\left\|\tilde{E}\right\|\right]\Big\}. \end{aligned} \tag{A6}$$

Then

$$\dot{V} \leq -Z_n^T\Phi Z_n + Z_n^T\Psi \tag{A7}$$

where Φ and Ψ are described in (16a)–(20). It is assumed that $\dot{V} \leq -\lambda Z_n^TZ_n$, where $\lambda > 0$. For the positive definite of $\Phi - \lambda I$, its principal minor must be greater than zero, i.e.,

if

$$\phi_{11} - \lambda > 0$$

then

$$|\sigma| > [\varepsilon(1 + k_0) - \xi_2]/(\xi_1 - \varepsilon k_1 - \lambda) \tag{A8}$$

if

$$\begin{vmatrix}\phi_{11} - \lambda & \phi_{12}\\ \phi_{12} & \phi_{22} - \lambda\end{vmatrix} > 0$$

then

$$\begin{aligned}|\sigma| > &[\varepsilon(1 + k_0) - \xi_2]/[4(\eta_1 - \lambda)]/\\ &\{\xi_1 - \varepsilon k_1 - \lambda - \varepsilon^2k_2^2/[4(\eta_1 - \lambda)]\}\end{aligned} \tag{A9}$$

if

$$\begin{vmatrix}\phi_{11} - \lambda & \phi_{12} & 0\\ \phi_{12} & \phi_{22} - \lambda & 0\\ 0 & 0 & \phi_{33} - \lambda\end{vmatrix} > 0$$

then

$$(\phi_{33} - \lambda)[(\phi_{11} - \lambda)(\phi_{22} - \lambda) - \phi_{12}^2] > 0 \tag{A10}$$

and if

$$|\Phi - \lambda I| > 0$$

then

$$|\sigma| > \varepsilon(1 + k_0) - \xi_2/q. \tag{A11}$$

From (A8)–(A11) and the condition (16a)–(16c), the result to accomplish $\Phi \geq \lambda I$ is $|\sigma| \geq 0$. Together with the condition (16a)–(16c), $\dot{V} + \lambda Z_n^TZ_n \leq -Z_n^T[(\Phi - \lambda I)Z_n - \Psi] \leq 0$ is achieved. Then $\{\sigma, \tilde{W}_1, \tilde{W}_2, \tilde{E}\}$ are bounded and $\lim_{t\to\infty} Z(t) \in \overline{\Omega} = \{Z \in \Omega' | (\Phi - \lambda I)Z_n - \Psi = 0\}$. Then $\{\hat{\sigma}, \hat{W}_1, \hat{W}_2, \hat{E}, u\}$ are bounded and then $\{x\}$ is bounded. Finally, if the condition $|\sigma| \leq \alpha$ is satisfied, based on Lemma 1, $\|\overline{E}\| < K_1\alpha/K_2$.

Appendix B
The Parameter Values of Four-Bar-Linkage System

$$M_e(\theta_2) = J_m + G_1 + r_1^2G_2 + r_1\cos(\theta_2 - \theta_3)G_3 + r_2^2G_4 \tag{B1}$$

$$C_b(\theta_2) = r_1 q_1 G_2 + [q_1 \cos(\theta_2 - \theta_3) - r_1(1 - r_1)\sin(\theta_2 - \theta_3)]G_3/2 + r_2 q_2 G_4 \tag{B2}$$

$$G_1 = m_2 z_2^2 + I_2 + m_3 l_2^2, \qquad G_2 = m_3 l_3^2/4 + I_3, \qquad G_3 = m_3 l_2 l_3, \qquad G_4 = m_4 l_4^2/4 + I_4 \tag{B3}$$

$$q_1 = [-l_4 r_2^2 + l_2 \cos(\theta_2 - \theta_4) + l_3 r_1^2 \cos(\theta_3 - \theta_4)]/[l_4 \sin(\theta_4 - \theta_3)] \tag{B4}$$

$$q_2 = [-l_3 r_1^2 - l_2 \cos(\theta_2 - \theta_3) + l_4 r_2^2 \cos(\theta_4 - \theta_3)]/[l_4 \sin(\theta_3 - \theta_4)] \tag{B5}$$

$$r_1 = l_2 \sin(\theta_2 - \theta_4)/[l_3 \sin(\theta_4 - \theta_3)], \qquad r_2 = l_2 \sin(\theta_2 - \theta_3)/[l_4 \sin(\theta_4 - \theta_3)] \tag{B6}$$

$$\theta_i = 2\tan^{-1}\left[-\left(b_i + \sqrt{b_i - 4a_i c_i}\right)\Big/(2a_i)\right], \qquad a_i = [1 + (-1)^{i+1} k_{i2}]\cos(\theta_2) + k_{i3} - k_{i1}, \qquad i = 3,\ 4 \tag{B7}$$

$$b_i = -2\sin(\theta_2), \qquad c_i = -[1 + (-1)^i k_{i2}]\cos(\theta_2) + k_{i3} + k_{i1}, \qquad i = 3,\ 4 \tag{B8}$$

$$k_{i1} = l_1/l_2, \qquad k_{i2} = l_1/l_i, \qquad k_{i3} = [l_4^2 - l_3^2 + (-1)^i (l_2^2 + l_1^2)]/(2 l_2 l_i), \qquad i = 3,\ 4. \tag{B9}$$

ACKNOWLEDGMENT

The authors would like to thank the reviewers and associate editor for their comments.

REFERENCES

[1] Albus, "A new approach to manipulator control: The cerebella model articulation controller (CMAC)," *Trans. ASME, J. Dyna. Syst., Measurement, Contr.*, vol. 63, no. 3, pp. 220–227, 1975.

[2] K. S. Narendra and K. Parthasarathy, "Identification and control of dynamical systems using neural networks," *IEEE Trans. Neural Networks*, vol. 1, pp. 4–27, 1990.

[3] R. M. Sanner and J.-J. E. Slotine, "Gaussian networks for direct adaptive control," *IEEE Trans. Neural Networks*, vol. 3, pp. 837–863, 1992.

[4] C. C. Ku and K. Y. Lee, "Diagonal recurrent neural networks for dynamic systems control," *IEEE Trans. Neural Networks*, vol. 6, pp. 144–156, 1995.

[5] S. I. Mistry, S. L. Chang, and S. S. Nair, "Indirect control of a class of nonlinear dynamic systems," *IEEE Trans. Neural Networks*, vol. 7, pp. 1015–1023, 1996.

[6] G. A. Rovithakis and M. A. Christodoulou, "Neural adaptive regulation of unknown nonlinear dynamical systems," *IEEE Trans. Syst., Man, Cybern. B*, vol. 27, pp. 810–822, 1997.

[7] C. L. Hwang, "Neural-network-based variable structure control for electrohydraulic servosystems subject to huge uncertainties without persistent excitation," *IEEE/ASME Trans. Mechatron.*, vol. 4, pp. 50–59, 1999.

[8] S. Seshagiri and H. K. Khalil, "Output feedback control of nonlinear systems using RBF neural networks," *IEEE Trans. Neural Networks*, vol. 11, pp. 69–79, 2000.

[9] Y. K. Kim and F. L. Lewis, "Reinforcement adaptive learning neural-net-based friction compensation control for high speed and precision," *IEEE Trans. Contr. Syst. Technol.*, vol. 8, pp. 118–126, Jan. 2000.

[10] C. L. Hwang and C. H. Lin, "A discrete-time multivariable neuro-adaptive control for nonlinear unknown dynamic systems," *IEEE Trans. Syst., Man, Cybern. B*, vol. 30, pp. 865–877, 2000.

[11] C. L. Hwang, "Neuro-adaptive variable structure control with multi-function for nonlinear systems," in *36th IEEE Conf. Decision Contr.*, San Diego, CA, Dec. 10–12, 1997, pp. 3249–3253.

[12] Y. Hung, W. Gao, and J. C. Hung, "Variable structure control: A survey," *IEEE Trans Ind. Electron.*, vol. 40, pp. 2–22, 1993.

[13] K. D. Young, V. I. Utkin, and Ü. Özgüner, "A control engineer's guide to sliding mode control," *IEEE Trans. Contr. Syst. Technol.*, vol. 7, pp. 328–342, May 1999.

[14] K. Furuta and Y. Pan, "Variable structure control with sliding sector," *Automatica*, vol. 36, no. 3, pp. 211–228, 2000.

[15] M. Vidyasagar, *Nonlinear Systems Analysis*, 2nd ed. Englewood Cliffs, NJ: Prentice-Hall, 1993.

[16] H. K. Khalil, *Nonlinear Systems*, 2nd ed. Englewood Cliffs, NJ: Prentice-Hall, 1996.

[17] J. T. Teeter, M. Y. Chow, and J. J. Brickley, "A novel fuzzy friction compensation approach to improve the performance of a dc motor control system," *IEEE Trans. Ind. Electron.*, vol. 43, pp. 113–120, 1996.

[18] W. J. Zhang, Q. Li, and L. S. Guo, "Integrated design of mechanical structure and control algorithm for a programmable four-bar linkage," *IEEE/ASME Trans. Mechatron.*, vol. 4, pp. 354–362, 1999.